# An Online Secondary Path Modeling Technique in a Hybrid Active Noise Control System

Harold Alexis Lao* and Cheng-Yuan Chang
* University of Santo Tomas, Philippines
E-mail: halao@ust.edu.ph Tel: +63-2-3406-1611
Chung Yuan Christian University, Taiwan
E-mail: ccy@cycu.edu.tw Tel: +886-3-2654838

*Abstract*— **This paper proposes an improved hybrid active noise control (HANC) system with online secondary path modeling (OSPM) technique by introducing three key enhancements from an earlier work. First, the desired signal of the cascading filter is changed to the modeling error. Second, an auxiliary noise power scheduling is added to adjust the injected noise dynamically. Third, a variable step-size (VSS) strategy is also added for fast convergence and robust performance. A refreshment scheme is also employed to maintain stability after sudden changes in the secondary path. Simulation results show that the proposed system outperforms existing methods in terms of noise reduction, convergence speed, and modeling accuracy, while maintaining stability after sudden changes in the environment.**

## I. INTRODUCTION

Active noise control (ANC) is a technology that relies on the principle of superposition to generate an anti-noise signal to cancel the unwanted noise [1][2]. It is effective at reducing low-frequency acoustic noise when passive means become bulky and impractical to use. ANC technology can be found in applications, such as in a headrest [3], fan [4], and pillow [5].

A hybrid ANC (HANC) system combines both feedforward feedback ANC systems into a single structure to deal with two uncorrelated noise sources. Some real-world applications of HANC systems are in a room [6], duct [7], hearing protection [8], and infant incubator [9].

The filtered-x LMS (FxLMS) algorithm is the most common adaptive algorithm used in ANC systems, which relies on estimating the secondary path transfer function to compensate for the secondary path effects [2]. This model is usually obtained offline and then used during the ANC operation. However, in practical applications, the secondary path can change, such as when someone using an ANC headset adjusts its position for comfort [10], causing the earcups to move closer or further from the ear. In this case, online secondary path modeling (OSPM) is required to ensure the stability and convergence of the ANC system [11].

An earlier work on hybrid ANC system with OSPM [12] used an auxiliary white noise to model the secondary path estimate and applies the variable step-size (VSS) approach of [13]. Another approach [14] added an OSPM system to the HANC with cascading filter [15]. However, both methods use a fixed auxiliary noise variance, degrading the system's steady-state noise reduction performance. Finally, a linear prediction filter (LPF) is proposed [16] to separate the broadband and narrowband components of the residual noise while controlling the auxiliary noise gain from the outputs of the cascading filter and the LPF. While the system yields significant performance improvements, the LPF introduces computational complexity and more parameters to tune.

This paper proposes an online secondary path modeling technique for a single-channel HANC system. It utilizes a VSS strategy for OSPM and introduces a large auxiliary noise gain at the start and then reduces to a very small value near steady state, resulting in fast convergence and good noise reduction. These strategies can potentially benefit spatial ANC when expanded to multi-channel ANC systems, which use multiple sensors and loudspeakers to reduce noise over a region.

## II. REVIEW OF EXISTING HANC SYSTEM

Figure 1 shows the HANC system with cascading filter and OSPM [14]. Compared to a traditional HANC system, this system utilizes an additional adaptive filter, known as the cascading or supporting filter $H(z)$, at the presence of uncorrelated narrowband disturbance $v_p(n)$. The purpose of $H(z)$ is to use its output $y_h(n)$ and error $e_h(n)$ signals to update the control filter coefficients $W_1(z)$ and $W_2(z)$ of the feedforward and feedback stages, respectively, resulting in

979-8-3315-7206-8/25/$31.00  

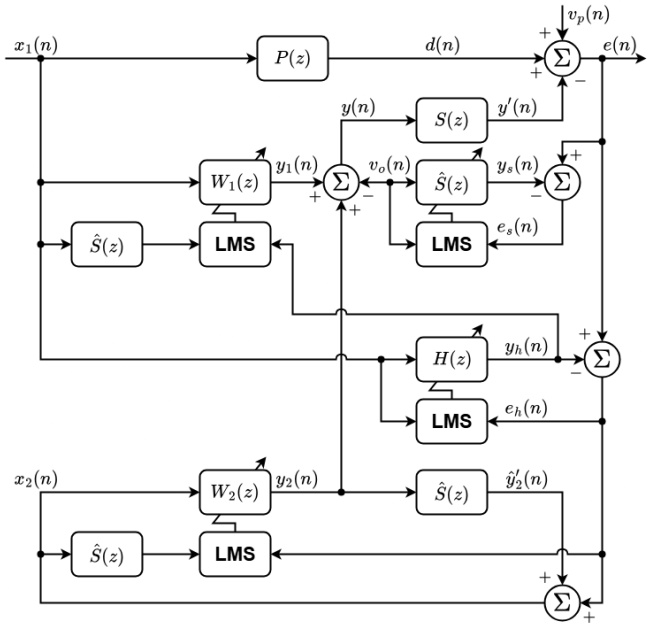


Fig. 1 Block diagram of HANC system with cascading filter and OSPM [14]

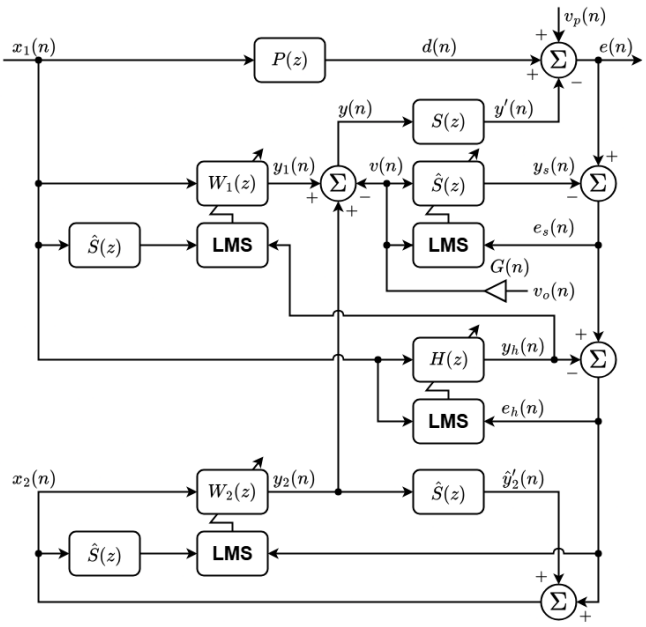


Fig. 2 Block diagram of the proposed HANC system

better noise reduction and faster convergence speed. The reference signal $x_2(n)$ is internally generated from $e_h(n)$ and the filtered secondary signal $\hat{y}'_2(n)$. The coefficients of $W_1(z)$ and $W_2(z)$ are updated using the FxLMS algorithm, while the adaptation of $H(z)$ uses the standard LMS algorithm.

The system also has an OSPM system to make it adapt to changes caused by physical and environmental factors. An auxiliary white noise $v_o(n)$ with zero-mean and variance $\sigma_o^2$ serves as the input to the OSPM. The modeling error $e_s(n)$ is obtained by subtracting the OSPM output $y_s(n)$ from $e(n)$, which is then used to update the coefficients of $\hat{S}(z)$ via the LMS algorithm. The main problem of this method is the lack of control in $\sigma_o^2$, which can degrade its steady-state noise reduction performance. A large $\sigma_o^2$ causes fast convergence of the OSPM at the expense of worse noise reduction, while a small $\sigma_o^2$ leads to slow convergence and less robust to changes in the acoustic paths. Thus, noise power scheduling achieves a tradeoff between fast convergence speed and good noise reduction.

## III. Proposed OSPM Technique For HANC Systems

The block diagram of the proposed algorithm is shown in Fig. 2, wherein desired signal to $H(z)$ is changed from the residual noise $e(n)$ to the modeling error $e_s(n)$, and the auxiliary noise power $\sigma_o^2$ is controlled by a variable gain $G(n)$. It also uses a simple variable step-size technique based on the ratio of the powers of the error signals. Finally, an existing refreshment scheme that resets the filters and first-order estimates right after sudden changes in the environment to ensure stability.

### *A. Desired Signal for the Cascading Filter*

In the proposed method shown in Fig. 2, the modeling error $e_s(n)$ serves as the desired signal to the cascading filter $H(z)$. The expression for the residual noise $e(n)$ is given as

$$e(n) = d(n) + v_p(n) - y'(n) \tag{1}$$

where $d(n)$ is the primary noise, $v_p(n)$ is the uncorrelated narrowband disturbance and $y'(n)$ is the filtered secondary signal. Also,

$$d(n) = p(n) * x_1(n) \tag{2}$$
$$y'(n) = s(n) * y(n) \tag{3}$$

where $p(n)$ and $s(n)$ are the primary and secondary path impulse responses, respectively, $x_1(n)$ as the reference signal, and $y(n)$ is the secondary signal given as

$$y(n) = y_1(n) + y_2(n) - v(n) \tag{4}$$

where $y_1(n)$ and $y_2(n)$ are the control filter outputs of the feedforward and feedback stages, respectively, and $v(n)$ is the auxiliary noise $v_o(n)$ scaled by the gain $G(n)$ given as

$$v(n) = G(n)v_o(n) \quad (5)$$

Substituting (3) and (4) into (1),

$$e(n) = d(n) + v_p(n) - s(n) * [y_1(n) + y_2(n)] + s(n) * v(n) \quad (6)$$

Next, the OSPM output $y_s(n)$ with an expression of

$$y_s(n) = \hat{s}(n) * v(n) \quad (7)$$

where $\hat{s}(n)$ is the impulse response of the secondary path estimate filter, is then subtracted from $e(n)$ to get $e_s(n)$,

$$e_s(n) = e(n) - y_s(n) = e(n) - \hat{s}(n) * v(n) \quad (8)$$

Substituting (6) into (8), the expression for $e_s(n)$ is given as

$$e_s(n) = d(n) + v_p(n) - s(n) * [y_1(n) + y_2(n)] + [s(n) - \hat{s}(n)] * v(n) \quad (9)$$

If $\hat{s}(n) \approx s(n)$, then (9) simplifies to the expression of the error signal of Fig. 1 (i.e., as if the OSPM system is not present), which is also the desired signal for $H(z)$. Although the value of $\hat{s}(n)$ may be far from that of $s(n)$ during the initial stages of adaptation, but a large initial auxiliary noise gain ensures fast convergence.

### *B. Auxiliary Noise Power Gain*

The auxiliary noise gain for the proposed method based on [17] and is given as

$$G(n+1) = \sqrt{\frac{P_e(n)}{[r(n)+1]P_s(n)}} \quad (10)$$

where $r(n)$ is the ratio of the power of the residual noise with disturbance and the power of the auxiliary noise [18], and the powers $P_e(n)$ and $P_s(n)$ are estimated as

$$P_e(n) = \lambda P_e(n-1) + (1-\lambda)e^2(n) \quad (11)$$

$$P_s(n) = \lambda P_s(n-1) + (1-\lambda)\hat{\mathbf{s}}^T(n)\hat{\mathbf{s}}(n) \quad (12)$$

where $\lambda$ is the forgetting factor close to unity and $\hat{\mathbf{s}}(n)$ is the vector of coefficients of the secondary path estimate. The expression of $r(n)$ is set to

$$r(n) = \max(k_r\, P_d(n)/P_e(n),\ 1) \quad (13)$$

where $k_r$ is a constant, $P_d(n)$ is the estimated power of the primary noise with the uncorrelated disturbance given as

$$P_d(n) = \lambda P_d(n-1) + (1-\lambda)\hat{d}^2(n) \quad (14)$$

and the estimate $\hat{d}(n)$ is generated by

$$\hat{d}(n) \approx \hat{\mathbf{s}}(n) * y(n) + e_s(n) \quad (15)$$

With the expression in (13), the value of $r(n)$ is equal to one during the initial stages of adaptation until such time that the approximate noise reduction $P_d(n)/P_e(n)$ is greater than $1/k_r$, at which the value of $r(n)$ increases rapidly, causing the gain expression in (10) to decrease heavily. Thus, the injected auxiliary noise to the system is initially large and then decreases rapidly towards steady state when the noise reduction is significant.

### *C. Variable Step Size*

The proposed method uses a simple VSS technique to improve system performance. The expression of the step size of the OSPM system is given as

$$\mu_s(n) = \rho(n)\mu_{s_{\max}} \quad (16)$$

where $\rho(n)$ is the ratio of powers utilized by OSPM systems [13], [19] with an expression of

$$\rho(n) = P_{e_s}(n)/P_e(n) \quad (17)$$

where the numerator is the power of the modeling error

$$P_{e_s}(n) = \lambda P_{e_s}(n-1) + (1-\lambda)e_s^2(n) \quad (18)$$

and $\mu_{s_{\max}}$ is the maximum step size value.

The behavior of the VSS strategy in (16) is as follows [19]. Initially, the step size value is at a maximum since the estimated powers are initialized to one. A large initial auxiliary noise gain in (10) causes the OSPM system to converge rapidly, resulting in the power of the modeling error and the ratio $\rho(n)$ in (17) to decrease. When $\hat{s}(n) \approx s(n)$ is achieved, the gain $G(n)$ suddenly decreases to a very small value, causing the power of the residual noise to decrease. Therefore, at steady state, the ratio $\rho(n)$ in (17) approaches unity, making the step size in (16) increase towards the maximum value, which

improves its responsiveness to sudden changes in the environment. This VSS strategy is desirable to prevent instability at the early stage of adaptation while allowing a larger steady-state step size compared to using a fixed value.

### D. Refreshment Scheme

Although the proposed system is relatively robust, it may converge to a sub-optimal state after a sudden change in the acoustic paths or the reference signal. Therefore, a refreshment scheme that detects sudden changes and then re-initializes all adaptive filters and other parameters is important to ensure the best performance. The method in [16] is applied to the proposed method, which takes the smoothed average of $P_e(n)$ over a time window $T_p$ given as

$$P_{e,T}(n') = \lambda P_{e,T}(n'-1) + (1-\lambda)\sum_{k=0}^{T_p-1} P_e(n'T_p - k) \quad (19)$$

where $n'$ is also a positive integer. The system is refreshed and re-initialized if the following condition is met:

$$P_{e,T}(n') \geq \alpha P_{e,T}(n'-1) \quad (20)$$

where $\alpha$ is a constant a little above one. Based on experience in using the proposed algorithm, the estimated power signals in (11), (12), (14), and (18) are also re-initialized to make the system more robust to sudden system changes, and the values of $\alpha$ and $T_p$ are tuned to obtain stable results.

## IV. Computational Complexity

A comparison of the number of mathematical operations required per iteration among the various systems is given in Table I, where $L_1$ and $L_2$ are the control filter lengths, $L_{sh}$ is the filter length of $\hat{S}(z)$, and $L_h$ is the filter length of $H(z)$. The proposed system requires additional $2L_{sh}+15$ multiplications, $2L_{sh}+4$ additions, three divisions and one square root operation compared to the existing method. Computing $P_s(n)$ and $\hat{d}(n)$ mainly contributes to this burden, especially for large values of $L_{sh}$.

TABLE I. Computational Complexity Comparison

| | Number of Operations per Iteration | | | |
|---|---|---|---|---|
| | × | + | ÷ | √ |
| Padhi's method [14] | $2L_1+2L_2+5L_{sh}+2L_h+4$ | $2L_1+2L_2+5L_{sh}+2L_h-2$ | 0 | 0 |
| Proposed method | $2L_1+2L_2+7L_{sh}+2L_h+19$ | $2L_1+2L_2+7L_{sh}+2L_h+2$ | 3 | 1 |

## V. Simulation Results

This section presents the simulation results to verify the effectiveness of the proposed method relative to the HANC with cascading filter without OSPM (referred to as the Akhtar's method [15]) and with OSPM (referred to as Padhi's method [14]). Tests are performed using two sets of simulation conditions as shown in Table II, with a sampling frequency of 2 kHz. A zero-mean white noise with variance of 0.01 is added as measurement noise, and the simulation results are obtained by averaging the results from 20 independent runs. The power of $v_p(n)$ is rescaled to match that of $d(n)$. The systems are compared in terms of the mean squared error (MSE) of the residual noise, and the relative modeling error (RME). The formulas are given as

TABLE II. Simulation Conditions

| | **Case 1** | **Case 2** |
|---|---|---|
| Input signal $x_1(n)$ | Zero-mean WN with $\sigma^2=1$ | Filtering a zero-mean WN with $\sigma^2=1$ through a BPF of order 128 with passband of 50-150 Hz |
| Uncorrelated disturbance $v_p(n)$ | Narrowband components at {100, 150, 200} Hz, amplitudes of {1, 0.5, 0.25} and phase angles of $\{0, \pi/6, \pi/3\}$ | Narrowband components at {100, 125} Hz, amplitudes of {1, 1} |
| Auxiliary noise $v_o(n)$ | Zero-mean WN with $\sigma_o^2=0.25$ (Padhi) and $\sigma_o^2=1$ (proposed) | |
| Primary path $P(z)$ | Lowpass filter using fir1 with cutoff at 600 Hz and $L_p=61$ | Approximated FIR filter from [1] and $L_p=256$ |
| Secondary path $S(z)$ | Lowpass filter using fir1 with cutoff at 600 Hz $L_s=31$ (first half) and $L_s=33$ (second half) | Approximated FIR filter from [1] and $L_s=64$ (first half) and two-sample right circular shift (second half) |
| Control filters $W_1(z)$ and $W_2(z)$ | $L_1=71,\ L_2=30,\ \mu_1=\mu_2=7.5\times10^{-4}$ | $L_1=L_2=100,\ \mu_1=2\times10^{-5},\ \mu_2=1\times10^{-5}$ |
| Cascading filter $H(z)$ | $L_{\mathrm{h}}=71,\ \mu_{\mathrm{h}}=1\times10^{-3}$ | $L_{\mathrm{h}}=100,\ \mu_{\mathrm{h}}=2.5\times10^{-3}$ |
| OSPM filter $\hat{S}(z)$ | $L_{\mathrm{sh}}=41,\ \mu_s=5\times10^{-4}$ (Padhi) and $\mu_{s_{\max}}=2.5\times10^{-3}$ (proposed) | $L_{\mathrm{sh}}=64,\ \mu_s=1.25\times10^{-4}$ (Padhi) and $\mu_{s_{\max}}=1.25\times10^{-2}$ (proposed) |
| Other parameters | $T_p=50,\ \alpha=1.1,\ k_r=0.75,\ \lambda=0.99$ (proposed) | |

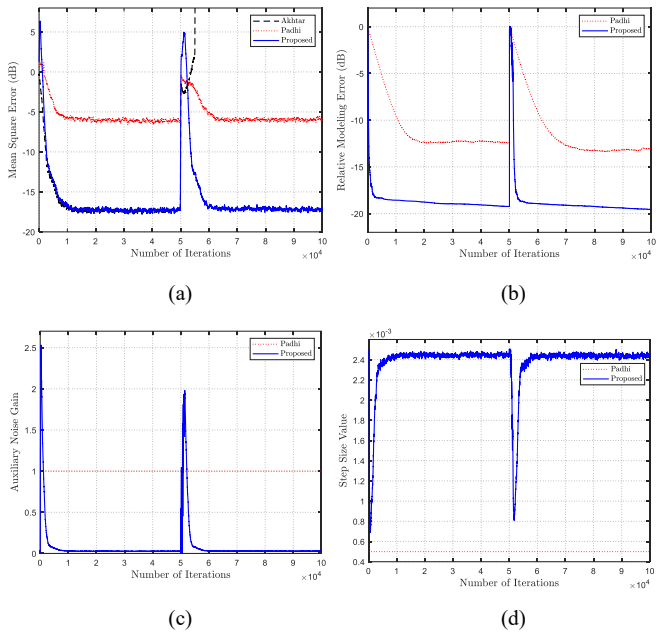


(a) (b) (c) (d)

Fig. 3 Simulation results for case 1 (a) Mean square error (MSE) (dB), (b) Relative modeling error (dB), (c) Auxiliary noise gain, (d) VSS for OSPM

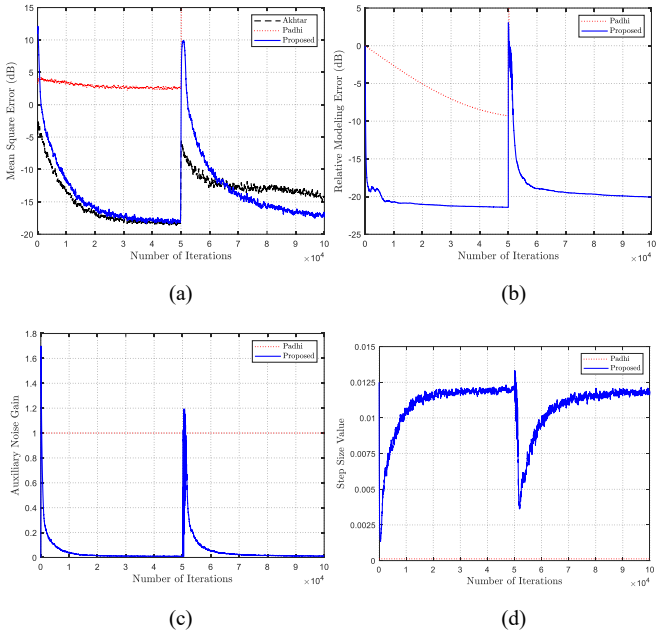


(a) (b) (c) (d)

Fig. 4 Simulation results for case 2 (a) Mean square error (MSE) (dB), (b) Relative modeling error (dB), (c) Auxiliary noise gain, (d) VSS for OSPM

$$\text{MSE (dB)} = 10\log_{10} E\{e^2(n)\} \quad (21)$$

$$\text{RME (dB)} = 20\log_{10}(\|\mathbf{s}(n) - \hat{\mathbf{s}}(n)\|/\|\mathbf{s}(n)\|) \quad (22)$$

where $\|\cdot\|$ is the Euclidean norm. Note that in (22), if the lengths of $\hat{\mathbf{s}}(n)$ and $\mathbf{s}(n)$ are not equal, zeros are padded to make the operation valid. For the proposed method, the plots of the variable noise gain and the OSPM step size will also be presented and analyzed. Finally, the secondary path is suddenly changed at the middle of the simulations to test how each system responds to environmental changes.

### *A. Case 1*

The simulation conditions of case 1 are based on [16], wherein the fir1 function from the MATLAB Signal Processing Toolbox is used to generate the acoustic paths. In Fig. 3(a), the proposed algorithm has very similar noise reduction to Akhtar's method but outperforms Padhi's method in terms of the relative modeling error, as shown in Fig. 3(b). This is due to the noise power scheduling of the proposed method shown in Fig. 3(c), wherein a large auxiliary noise is injected at the start to speed up the modeling process, resulting in a large peak error in Fig. 3(a) and a rapid decrease in the modeling error in Fig. 3(b). The gain then decreases to a very small value, yielding a good steady-state noise reduction performance and a minor improvement in the modeling error. Finally, Fig. 3(d), shows the behavior of the VSS technique used by the proposed method, with the initial value equal to the maximum, suddenly decreases when the gain is at its largest, and then rises back up towards the maximum value when the modeling error is low.

After introducing a change in the secondary path at the middle of the simulations, Akhtar's method becomes unstable as shown in Fig. 3(a) while the remaining methods are robust enough to remain stable. The simulation results in Fig. 3 show that the refreshment scheme was able to detect the change in path, allowing the system to re-initialize and obtain a similar performance right before the system is perturbed.

### *B. Case 2*

The simulation results for case 2 are shown in Fig. 4. Like case 1, Fig. 4(a) and Fig. 4(b) illustrate the improved noise reduction performance and relative modeling error, respectively, of the proposed method compared to Padhi's method. The large peak error at the initial stages of the simulation in Fig. 4(a) by the proposed method is due to the large initial gain in Fig. 4(c), which leads to a very steep decline of the modeling error shown in Fig. 4(b). If needed, the gain can be set to a maximum value to prevent damaging the physical components during implementation. The step size of the OSPM system shown in Fig. 4(d) behaves similarly to case 1.

After a sudden change in the secondary path, Fig. 4(a) and Fig. 4(b) show that Padhi's method becomes unstable, while Akhtar's method converged to a worse mean square error at

steady state. The refreshment scheme also detected the change and resets the system and then performed similarly at the point before the secondary path is changed.

## VI. Conclusion

In this paper, a new HANC system is proposed by applying several improvements to the HANC system with cascading filter and OSPM. First, the desired signal to the cascading filter is changed to the modeling error, which serves as the residual noise when the OSPM system is not present. Second, auxiliary noise power scheduling and VSS techniques are introduced to achieve better noise reduction performance and relative modeling error. Finally, a refreshment scheme from an earlier work makes the system more robust to sudden changes in the secondary path. Simulation results show that the proposed method has better noise reduction, convergence speed, and relative modeling error compared to existing approaches.

Future research can focus on reducing the computational cost, making it more practical for real-world hardware deployment. Another possible direction is the extension to multi-channel and 3D HANC systems to deal with more complex acoustic environments. Finally, the proposed system may be combined with the LPF [16] to further improve its performance.

## References


[1] S. M. Kuo and D. R. Morgan, *Active Noise Control Systems – Algorithms and DSP Implementation*. New York, NY, USA: Wiley, 1996.

[2] S. M. Kuo and D. R. Morgan, "Active noise control: a tutorial review," *Proc. IEEE*, vol. 87, no. 6, pp. 943–973, Jun. 1999.

[3] X. Shen, D. Shi, S. Peksi, and W.-S. Gan, "Implementations of wireless active noise control in the headrest," *Proc. INTER-NOISE Noise-Con Congr. Conf.*, pp. 3445–3455, Feb. 2023.

[4] C.-Y. Chang, X.-W. Liu, and S. M. Kuo, "Active noise control for centrifugal and axial fans," *Noise Control Eng. J.,* vol. 68, no. 6, pp. 490–500, Nov. 2020.

[5] C. -Y. Chang, C. -N. Chiou and S. M. Kuo, "A complete design of smart pad that reduces snoring," *IEEE Trans. Consum. Electron.*, vol. 69, no. 3, pp. 649–656, Aug. 2023.

[6] W.-K. Tseng, B. Rafaely, and S. J. Elliott, "Combined feedback-feedforward active noise control of sound in a room," *J. Acoust. Soc. Amer.*, vol. 104, no. 6, pp. 3417–3425, Dec. 1998.

[7] E. Esmailzadeh, A. Alasty, and A. R. Ohadi, "Hybrid active noise control of a one-dimensional acoustic duct," *J. Vib. Acoust.*, vol. 124, no. 1, pp. 10–18, Apr. 2001.

[8] L. R. Ray, J. A. Solbeck, A. D. Streeter, and R. D. Collier, "Hybrid feedforward-feedback active noise reduction for hearing protection and communication," *J. Acoust. Soc. Amer.*, vol. 120, no. 4, pp. 2026–2036, Oct. 2006.

[9] L. Liu, K. Beemanpally, and S. M. Kuo, "Application of multi-channel hybrid active noise control systems for infant incubators," *Noise Control Eng. J.*, vol. 61, no. 2, pp. 169–179, Mar. 2013.

[10] T.-R. Chen, F.-H, Hwang, H.-W. Hsu, and C.-Y. Chang, "Adaptive active noise control system for secondary path fluctuation problem," *Int. J. Innov. Comput., Inf. Control*, vol. 8, no. 1(B), pp. 967–976, Jan. 2012.

[11] S. M. Kuo and D. Vijayan, "A secondary path modeling technique for active noise control systems," *IEEE Trans. Speech Audio Process.*, vol. 5, no. 4, pp. 374–377, Jul. 1997.

[12] E. Lopez-Gaudana, P. Betancourt, E. Cruz, M. Nakano-Miyatake and H. Perez-Meana, "A hybrid active noise cancelling with secondary path modeling," in *Proc. 51st Midwest Symp. Circuits Syst. (MWSCAS)*, Knoxville, TN, USA, 2008, pp. 277–280.

[13] M.T. Akhtar, M. Abe, M. Kawamata, "A new variable step size LMS algorithm-based method for improved online secondary path modeling in active noise control systems", *IEEE Trans. Audio, Speech, Lang. Process.*, vol. 14, no. 2, pp.720–726, Mar. 2006.

[14] T. Padhi, M. Chandra, and A. Kar, "Performance evaluation of hybrid active noise control system with online secondary path modeling," *Appl. Acoust.*, vol. 133, pp. 215–226, Apr. 2018.

[15] M. T. Akhtar and W. Mitsuhashi, "Improving performance of hybrid active noise control systems for uncorrelated narrowband disturbances," *IEEE Trans. Audio, Speech, Lang. Process.*, vol. 19, no. 7, pp. 2058–2066, Sept. 2011.

[16] Z. Wang, Y. Xiao, Y. Ma, L. Ma and K. Khorasani, "A new hybrid active noise control system with input-power-controlled online secondary-path modeling," *IEEE/ACM Trans. Audio, Speech, Lang. Process.*, vol. 32, pp. 3157–3170, Jun. 2024.

[17] P. A. C. Lopes and J. A. B. Gerald, "Auxiliary noise power scheduling algorithm for active noise control with online secondary path modeling and sudden changes," *IEEE Signal Process. Lett.*, vol. 22, no. 10, pp. 1590–1594, Oct. 2015.

[18] A. Carini and S. Malatini, "Optimal variable step-size NLMS algorithms with auxiliary noise power scheduling for feedforward active noise control," *IEEE Trans. Audio, Speech, Lang. Process.*, vol. 16, no. 8, pp. 1383–1395, Nov. 2008.

[19] S. Ahmed, M. T. Akhtar and X. Zhang, "Robust auxiliary-noise-power scheduling in active noise control systems with online secondary path modeling," *IEEE Trans. Audio, Speech, Lang. Process.*, vol. 21, no. 4, pp. 749–761, Apr. 2013.